NJC

PAPER

View Article Online
View Journal | View Issue

Cite this: *New J. Chem.*, 2018, **42**, 18850

Synthesis, characterisation, crystal structures and biological studies of palladium(II) complexes containing 5-(2-hydroxy-3-methoxy-phenyl)-2,4-dihydro[1,2,4]triazole-3-thione derivatives†

A. Shanmugapriya,[a] F. Dallemer[b] and R. Prabhakaran *[a]

Received 25th July 2018,
Accepted 9th October 2018

DOI: 10.1039/c8nj03714k

rsc.li/njc

A series of new Pd(II) complexes (**1–4**) were obtained from the reactions between $K_2[PdCl_4]$, 3-methoxy-salicylaldehyde-4(*N*)-substituted thiosemicarbazone [H_2L^1–H_2L^4] and 1,3-bis(diphenylphosphino)propane [dppp]. All the complexes were characterized by various spectroscopic techniques (IR, electronic, ^{1}H-NMR and ESI-MS). The crystal structures of complexes **2** and **4** have been determined by single crystal X-ray diffraction. The binding affinity and binding mode of the palladium complexes (**1–4**) towards calf-thymus (CT) DNA and BSA (Bovine Serum Albumin) were studied by using UV-vis and fluorescence emission spectroscopy. These results showed that the binding of the complexes to DNA is through electrostatic interaction and the quenching of the complexes is static. Further they cleaved supercoiled DNA pBR322 without any added external agents. The alterations in the secondary structure of BSA by the Pd(II) complexes were confirmed by synchronous and three dimensional fluorescence spectroscopy. The cytotoxicity of the complexes was evaluated by an MTT assay in the MCF-7 cell line and complex **3** exhibited significant activity (IC_{50} = 5.60 ± 0.04 μM), which was comparable with those of the other complexes. The morphological changes assessed by acridine orange and ethidium bromide staining revealed that the cell death occurred through apoptosis.

Introduction

Serious side-effects caused by cisplatin and its analogues, carboplatin and oxaliplatin, including nephrotoxicity and drug resistance by tumor cells, provide an incentive for the discovery of more efficient cytotoxic complexes with other transition metals.[1,2] Due to many similarities between Pt(II) and Pd(II), there is considerable interest in the study of palladium(II) complexes as anticancer drugs.[1,3] Coordination of the biologically active organic molecules as ligands to the transition metal ions shows promise in this field due to their unique ability to bind different biological targets.[1,4] The coordinated ligands play an important role in the anticancer activity of metallodrugs because they can modify key parameters such as reactivity and lipophilicity.[5]

The nature of multidentate ligands has a profound effect on the coordination chemistry of metal complexes and also the design and "tailoring" of the ligand properties can lead to innovative metal chemistry.[6,7] There has been special interest on thiosemicarbazone ligands in recent years due to their coordination versatility,[8–11] analytical uses[12] and pharmacological activity.[8–13] Thiosemicarbazones usually possess two nucleophilic centres namely N(3)–H and S–H in their thione or thiolate form and a polar double bond (C=N). There are two possibilities for intra molecular cyclisation to afford a 1,2,4-triazolidine-3-thione (I) ring, which is formed by the cyclic fusion of N(3)–H with C=N and a 1,3,4-thiadiazoline-2-amine (II) ring, which is formed through the cyclic fusion of S–H with C=N.[14]

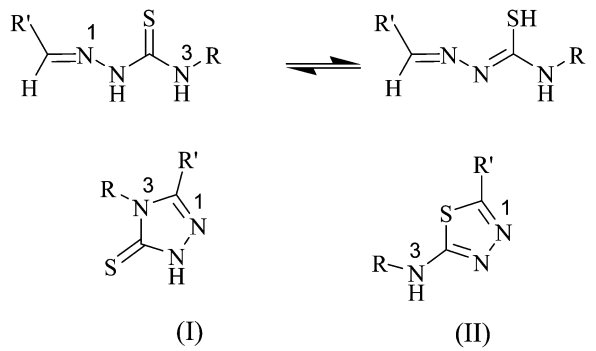

(I) (II)

In many cases, coordination of ligands to metal ions increases the bioactivity of compounds, suggesting that complexation is an

[a] *Department of Chemistry, Bharathiar University, Coimbatore 641 046, India. E-mail: rpnchemist@gmail.com; Fax: +91-422-2422387; Tel: +91-422-2428319*
[b] *Lab MADIREL CNRS UMR 7246, Aix Marseille University, Saint-Jerome Campus, MADIREL Bldg., 13397 Marseille Cedex 20, France*

† Electronic supplementary information (ESI) available. CCDC 1858145 and 1858146 contain the supplementary crystallographic data for complexes [Pd(H-Msal-mtsc)(Msal-mtaz)]·Cl (**2**) [Pd_2(Msal-ptsc)(Msal-ptaz)(H-Msal-ptsc)(Msal-ptaz)]·Cl (**4**) respectively. For ESI and crystallographic data in CIF or other electronic format see DOI: 10.1039/c8nj03714k

interesting strategy for dose reduction.[15–18] Salicylaldehyde thiosemicarbazones are derived from the incorporation of three donor atoms [O, N, and S], increasing the coordination capacity of the thiosemicarbazones upon coordination. Metal complexes of salicylaldehyde thiosemicarbazones have been studied for their *in vitro* antitumor activity, and in some cases, they were found to be generally more active than free ligands.[19,20] A number of palladium(II) thiosemicarbazone complexes have been synthesised and examined for their potential as antitumor agents.[2,21–25]

Generally, anticancer agents damage DNA or block DNA synthesis indirectly through inhibition of the biosynthesis of nucleic acid precursors, or by disrupting the hormonal stimulation of cell growth.[26] Therefore, investigations on the interaction of DNA with suitable molecules are very important for designing new types of pharmaceutical molecules. In addition, metal complexes that bind and cleave DNA or proteins under physiological conditions are of current interest owing to their varied applications in nucleic acid and protein chemistry.[27–30]

In this paper, we reported the derivatives of 3-5-(2-hydroxy-3-methoxy-phenyl)-2,4-dihydro[1,2,4]triazole-3-thione and their corresponding Pd(II) complexes (**1–4**) were synthesized and characterized by various spectroscopic techniques and their DNA/BSA binding, DNA cleavage, cytotoxicity and apoptosis were studied.

Experimental

1,3-Bis(diphenylphosphino)propane was purchased from Sigma Aldrich Ltd. The ligands [$\mathbf{H_2L^{1-4}}$], the palladium precursor $K_2[PdCl_4]$ and palladium(II) complexes were synthesized according to the standard literature procedures.[24,31,32] All the reagents used were of analar grade, and were purified and dried according to the standard procedure.[33] Protein free calf thymus DNA (CT-DNA), ethidium bromide (EB), bovine serum albumin (BSA), and 3-(4,5-dimethylthiazol-2-yl)-2,5-diphenyl-tetrazoliumbromide (MTT) were purchased from Hi Media. Infrared spectra were measured using KBr pellets on a JASCO FT-IR 4100 instrument between 400 and 4000 cm^{-1}. The melting points were measured using a Lab India apparatus. The electronic spectra of the complexes were recorded in chloroform using a JASCO V-630 spectrophotometer in the 800–200 nm range. Emission spectra were recorded by using JASCO FP-6600 and JASCO FP-8300 spectrofluorimeters. ^{1}H-NMR spectra were recorded in DMSO at room temperature using a Bruker 400 MHz instrument, chemical shifts relative to tetramethylsilane. The mass spectra of complexes **1** and **3** were recorded in DMSO using a Waters Q-Tof Micro instrument. Single crystal data collection and correction for new Pd(II) complexes **2** and **4** were done at 293 K with a CCD kappa diffractometer using graphite monochromated Mo Kα (λ = 0.71073) radiation.[34] The structure solution was done by using SHEL-XTL-97[35] and refined by full matrix least squares on F^2 using SHEL-XTL-97.[36]

Preparation of complex 1

0.069 g (0.3063 mmol) of 3-methoxysalicylaldehyde-4(*N*)-thiosemicarbazone [H_2-Msal-tsc] was dissolved in dichloromethane (30 cm^3) and was added to $K_2[PdCl_4]$ (0.100 g, 0.3063 mmol) in hot methanol (30 cm^3). The mixture was refluxed for 10 min. To this, 0.063 g of 1,3-bis(diphenylphosphino)propane (0.1531 mmol) was added. After 5 h of refluxing, the reaction mixture was allowed to stand for 3 days at room temperature. A reddish brown solid formed was subjected to thin layer chromatography, where two spots were identified and isolated by silica gel column chromatography using a benzene–methanol solvent mixture. The light yellow band was eluted with 98 : 2 benzene–methanol, which afforded yellow crystals and it was identified to be $[PdCl_2(dppp)]$ and the light red band was eluted with a 90 : 10 benzene–methanol mixture and was crystallized by using a chloroform–ethylacetate mixture to afford a yellowish orange solid [(3-methoxysalicylaldehyde-thiosemicarbazone)(5-(2-hydroxy-3-methoxy-phenyl)-2,4-dihydro-[1,2,4]triazole-3-thione)palladium(II)] [Pd(H-Msal-tsc)(Msal-taz)]·Cl (**1**).

[$PdCl_2$(dppp)] (1a). Yield: 26%, m.p: > 250 °C; FT-IR (cm^{-1}) in KBr: 1465, 1094, 691 (for PPh_3); UV-vis. (DMSO), λ_{max} (nm) (dm^3 mol^{-1} cm^{-1}): 231 (62 795) (intra ligand transition); 313 (79 096) (LMCT); ^{1}H-NMR (DMSO-d_6 ppm): δ 1.19 (q, P–CH_2), δ 1.47 (m, –CH_2–), δ 7.46–7.53 (m, aromatic protons).

[Pd(H-Msal-tsc)(Msal-taz)]·Cl (1). Yield: 43%, m.p: 153 °C; FT-IR (cm^{-1}) in KBr: 3442 (ν_{OH}), 1595 ($\nu_{C=N}$), 846 and 964 ($\nu_{C=S}$); UV-vis. ($CHCl_3$), λ_{max} (nm) (dm^3 mol^{-1} cm^{-1}): 247 (62 318) (intra ligand transition) 304 (27 932), 340 (22 154), 401 (9925) (LMCT); ^{1}H-NMR (DMSO-d_6 ppm): δ 11.26 (s, –OH), δ 10.50 (s, NHC=S), δ 8.26 (s, –CH=N), δ 6.80 (t (J = 15.8), NH_2), δ 6.71–7.22 (m, aromatic protons), δ 6.55 (d (J = 7.4) triazole –N^2H), δ 6.47 (s, triazole –N^3H), δ 3.80 (s, –OCH_3); ESI-MS (DMSO), m/z value: 589.1237.

Preparation of complex 2

Complex **2** was prepared using the procedure described for complex **1**, with 3-methoxysalicylaldehyde-4(*N*)-methylthiosemicarbazone [H_2-Msal-mtsc], (0.073 g, 0.3063 mmol) dissolved in dichloromethane (30 cm^3), $K_2[PdCl_4]$ (0.100 g, 0.3063 mmol) and 1,3-bis(diphenylphosphino)propane (0.063 g, 0.1531 mmol). A reddish brown solid formed was subjected to thin layer chromatography, where two spots were identified and isolated by silica gel column chromatography using a benzene–methanol solvent mixture. The light yellow band was eluted with 98 : 2 benzene–methanol, which afforded yellow crystals and it was identified to be $[PdCl_2(dppp)]$ (**2a**) and the light red band was eluted with a 90 : 10 benzene–methanol mixture and was crystallized by using a chloroform–methanol mixture to afford red crystals of [(3-methoxysalicylaldehyde-4(*N*)-methylthiosemicarbazone)(5-(2-hydroxy-3-methoxy-phenyl)-4-methyl-2,4-dihydro-[1,2,4]triazole-3-thione)palladium(II)] [Pd(H-Msal-mtsc)(Msal-mtaz)]·Cl (**2**) suitable for X-ray crystallographic studies.

[$PdCl_2$(dppp)] (2a). Yield: 23%, m.p: > 250 °C; FT-IR (cm^{-1}) in KBr: 1465, 1094, 691 (for PPh_3); UV-vis. (DMSO), λ_{max} (nm) (dm^3 mol^{-1} cm^{-1}): 231 (62 795) (intra ligand transition); 313 (79 096) (LMCT); ^{1}H-NMR (DMSO-d_6 ppm): δ 1.19 (q, P–CH_2), δ 1.47 (m, –CH_2–), δ 7.46–7.53 (m, aromatic protons).

[Pd(H-Msal-mtsc)(Msal-mtaz)]·Cl (2). Yield: 46%, m.p: 175 °C; FT-IR (cm^{-1}) in KBr: 3422(ν_{OH}), 1590($\nu_{C=N}$), 821 and 1021($\nu_{C=S}$);

UV-vis. ($CHCl_3$), λ_{max} (nm) ($dm^3\ mol^{-1}\ cm^{-1}$): 247 (40 441) (intra ligand transition), 309 (20 793), 341 (16 671), 401 (8350) (LMCT); ^{1}H-NMR (DMSO-d_6 ppm): δ 12.05 (s, –OH), δ 10.48 (s, NHC═S), δ 9.69 (s, terminal –NH), δ 7.44 (d (J = 7.8), –CH═N), δ 6.66–7.39 (m, aromatic protons), δ 6.35 (s, triazole –N^{2}H), δ 3.81 (s, –OCH_3), δ 2.91 (s, –CH_3).

Preparation of complex 3

Complex **3** was prepared using the procedure described for complex **1**, with 3-methoxysalicylaldehyde-4(*N*)-ethylthiosemicarbazone [H_2-Msal-etsc] (0.077 g, 0.3063 mmol), $K_2[PdCl_4]$ (0.100 g, 0.3063 mmol) and 1,3-bis(diphenylphosphino)propane (0.063 g, 0.1531 mmol). A reddish brown solid formed was subjected to thin layer chromatography, where two spots were identified and isolated by silica gel column chromatography using a benzene–methanol solvent mixture. The light yellow band was eluted with 98 : 2 benzene–methanol, which afforded yellow crystals and it was identified to be [$PdCl_2$(dppp)] and the light red band was eluted with a 90 : 10 benzene–methanol mixture and was crystallized by using a chloroform–methanol mixture to afford red crystals of [(3-methoxysalicylaldehyde-4(*N*)-ethylthiosemicarbazone)(4-ethyl-5-(2-hydroxy-3-methoxyphenyl)-2,4-dihydro-[1,2,4]triazole-3-thione)palladium(II)] [Pd(H-Msal-etsc)(Msal-etaz)]·Cl (**3**).

[$PdCl_2$(dppp)] (3a). Yield: 28%, m.p: > 250 °C; FT-IR (cm^{-1}) in KBr: 1465, 1094, 691 (for PPh_3); UV-vis. (DMSO), λ_{max} (nm) ($dm^3\ mol^{-1}\ cm^{-1}$): 231 (62 795) (intra ligand transition); 313 (79 096) (LMCT); ^{1}H-NMR (DMSO-d_6 ppm): δ 1.19 (q, P–CH_2), δ 1.47 (m, –CH_2–), δ 7.46–7.53 (m, aromatic protons).

[Pd(H-Msal-etsc)(Msal-etaz)]·Cl (3). Yield: 43%, m.p: 189 °C; FT-IR (cm^{-1}) in KBr: 3436 (ν_{OH}), 1596 ($\nu_{C=N}$), 853 and 967 ($\nu_{C=S}$); UV-vis. ($CHCl_3$), λ_{max} (nm) ($dm^3\ mol^{-1}\ cm^{-1}$): 252 (18 517) (intra ligand transition), 320 (10 813), 405 (3218) (LMCT); ^{1}H-NMR (DMSO-d_6 ppm): δ 12.26 (s, –OH), δ 12.02 (s, NHC═S), δ 11.12 (s, terminal –NH), δ 7.71 (d (J = 8), –CH═N), δ 6.67–7.38 (m, aromatic protons), δ 6.38 (s, triazole –N^{2}H), δ 3.76 (s, –OCH_3), δ 2.88 (m, –CH_2), δ 1.26 (t (J = 12), –CH_3); ESI-MS (DMSO), m/z value: 645.2493.

Preparation of complex 4

Complex **4** was prepared using the procedure described for complex **1**, with methoxysalicylaldehyde-4(*N*)-phenylthiosemicarbazone [H_2-Msal-ptsc] (0.092 g, 0.3063 mmol), $K_2[PdCl_4]$ (0.100 g, 0.3063 mmol) and 1,3-bis(diphenylphosphino)propane (0.063 g, 0.1531 mmol). A reddish brown solid formed was subjected to thin layer chromatography, where two spots were identified and isolated by silica gel column chromatography using a benzene–methanol solvent mixture. The light yellow band was eluted with 98 : 2 benzene–methanol, which afforded yellow crystals and it was identified to be [$PdCl_2$(dppp)] and the light red band was eluted with a 90 : 10 benzene–methanol mixture and was crystallized by using a dichloromethane–methanol mixture to afford orange crystals of [(3-methoxy salicylaldehyde-4(*N*)-phenylthiosemicarbazone)(5-(2-hydroxy-3-methoxy-phenyl)-4-phenyl-2,4-dihydro-[1,2,4]triazole-3-thione)palladium(II)] [Pd_2(Msal-ptsc)-(Msal-ptaz)(H-Msal-ptsc)(Msal-ptaz)]·Cl (**4**) suitable for X-ray crystallographic studies.

[$PdCl_2$(dppp)] (4a). Yield: 25%, m.p: > 250 °C; FT-IR (cm^{-1}) in KBr: 1465, 1094, 691 (for PPh_3); UV-vis. (DMSO), λ_{max} (nm) ($dm^3\ mol^{-1}\ cm^{-1}$): 231 (62 795) (intra ligand transition); 313 (79 096) (LMCT); ^{1}H-NMR (DMSO-d_6 ppm): δ 1.19 (q, P–CH_2), δ 1.47 (m, –CH_2–), δ 7.46–7.53 (m, aromatic protons).

[Pd_2(Msal-ptsc)(Msal-ptaz)(H-Msal-ptsc)(Msal-ptaz)]·Cl (4). Yield: 48%, m.p: 210 °C; FT-IR (cm^{-1}) in KBr: 3418 (ν_{OH}), 1594 ($\nu_{C=N}$), 858 and 975($\nu_{C=S}$), 738 (ν_{C-S}); UV-vis. ($CHCl_3$), λ_{max} (nm) ($dm^3\ mol^{-1}\ cm^{-1}$): 246 (27 575) (intra ligand transition), 300 (14 068), 375 (4817), 400 (5825) (LMCT); ^{1}H-NMR (DMSO-d_6 ppm): δ 12.51 (s, –OH), δ 11.29 (s, NHC═S), δ 10.30 (s, terminal –NH), δ 7.95 (s, –CH═N), δ 6.29–7.69 (m, aromatic protons), δ 6.18 (d (J = 7.8), triazole –N^{2}H), δ 3.78(s, –OCH_3).

DNA binding studies

DNA binding studies were carried out according to the method described in the earlier reports.[24] Various concentrations of CT-DNA (5–50 μM) in Tris–HCl buffer (pH 7.2) were treated with complexes (**1–4**) (10 μM) in 1% aqueous DMSO. Detailed procedures for the DNA binding experiment are provided in the ESI.†

Competitive binding with ethidium bromide

Ethidium bromide studies were carried out according to the earlier reported methods.[24,25] Detailed procedures for the DNA binding experiments are provided in the ESI.†

DNA cleavage studies

The cleavage of DNA was monitored by using agarose gel electrophoresis[37] and the detailed procedure is given in the ESI.†

Bovine serum albumin binding studies

Protein binding studies were done according to the earlier reported methods[24,25] and are described in the ESI.†

Cytotoxicity studies

3-(4,5-Dimethylthiazol-2-yl)-2,5-diphenyltetrazolium bromide (MTT) assay[38]. The cytotoxic activity of the new palladium(II) complexes was evaluated and the IC_{50} values were determined from nonlinear regression using GraphPad Prism 5.[39] The observation of the morphological changes of the apoptotic cells was performed according to the method with slight modifications.[40] Acridine orange/ethidium bromide staining was carried out by the method of Gohel *et al.*[41] The experimental procedures are given in the ESI.†

Results and discussion

The reactions of 3-methoxysalicylaldehyde-4(*N*)-substituted thiosemicarbazone ($\mathbf{H_2L^{1-4}}$) with $K_2[PdCl_4]$ and 1,3-bis(diphenylphosphino)propane [dppp] in 1 : 1 methanol–dichloromethane resulted in the formation of new complexes **1–4** (Scheme 1), the analytical data of which confirmed their stoichiometry (**1–4**). The structures of complexes **2** and **4** were confirmed by X-ray crystallographic studies. These complexes are

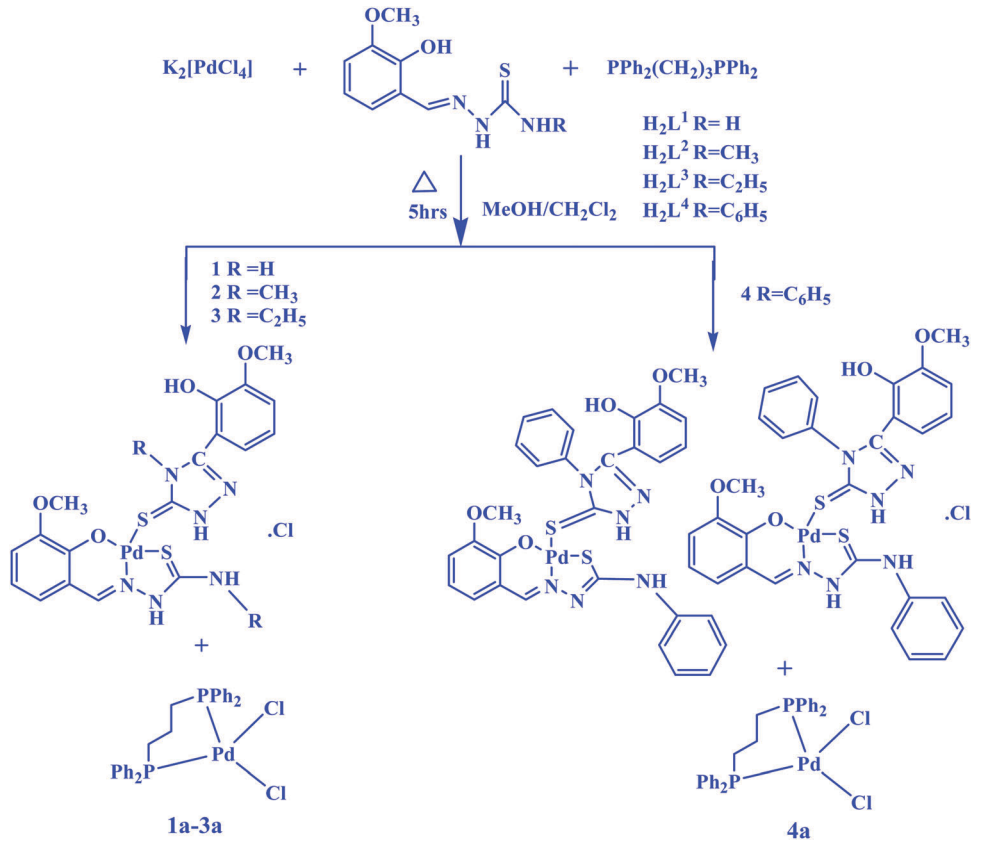

Scheme 1 Synthesis of new palladium(II) complexes.

soluble in common organic solvents such as dichloromethane, chloroform, ethanol, methanol, dimethylformamide and dimethylsulfoxide.

IR spectroscopy

A strong absorption at 1539–1593 cm^{-1} for the ligands [H_2L^{1-4}] corresponding to the presence of the $\nu_{(C=N)}$ group shifted to a higher frequency (1590–1596 cm^{-1}) for all the complexes, which can be attributed to the donation of a lone pair of the nitrogen to the metal during the coordination (Fig. S1–S5, ESI†).[24,42] A band in the region of 3310–3457 cm^{-1} was attributed to the presence of the –OH group of free ligands [H_2L^{1-4}] and this band was observed at 3418–3442 cm^{-1} for the complexes (**1–4**), suggesting the non-participation of phenolic OH in bonding. The absence of the $\nu_{(S-H)}$ stretching frequency in the region of 2500–2600 cm^{-1} and the presence of $\nu_{(N-H)}$ stretching frequency in the range of 3171–3258 cm^{-1} in the IR spectra of the metal complexes (**1–4**) indicate that the thione sulphur atom coordinated to the metal ion rather than thiolate. This is further inferred from the presence of a strong stretching frequency in the 772–788 cm^{-1} region due to the shift in the $\nu_{(C=S)}$ in the ligand to 821–853 cm^{-1} in the metal complexes (**1–3**).[43,44] Whereas in complex **4**, there were two signals at 858 cm^{-1} and 738 cm^{-1}, corresponding to the presence of $\nu_{(C=S)}$ and $\nu_{(C-S)}$, respectively,[25,43] and the reason for this observation became clear to us only after solving the X-ray single crystal structure of complex **4**.

Electronic spectroscopy

The electronic spectra of the palladium(II) complexes (**1–4**) were recorded in chloroform and they displayed three to four bands in the region around 246–405 nm (Fig. S6, ESI†). The bands appearing in the 246–252 nm region were assigned to the intra ligand transition.[45] The bands that were found around 300–405 nm were assigned to the ligand to metal charge transfer (LMCT) transitions (s → d).[46]

^{1}H-NMR spectroscopy

The ^{1}H-NMR spectra of the ligands and the complexes (**1–4**) were recorded in DMSO (Fig. S7–S11, ESI†). The spectrum of the ligands [H_2L^{1-4}] showed a singlet at δ 9.13–10.00 ppm corresponding to the (N(2)H–C═S) group.[24] However in complexes **1–4**, a singlet appeared at δ 10.48–12.02 ppm due to the (N(2)H–C═S–) group, indicating that the ligand remains in its thionic form.[47] This shift showed that the thiosemicarbazone coordinated to the palladium through the thione sulphur atom rather than thiolate sulphur.[48] In the ligands, a sharp singlet corresponding to the presence of phenolic –OH was found at δ 11.34–11.76 ppm. However, this peak was upfield shifted to δ 11.26–12.51 ppm in the complexes (**1–4**) indicating the non-participation of the phenolic oxygen in coordination.[49] In all the complexes, the aromatic protons of the coordinated ligands were found as a multiplet at δ 6.19–7.95 ppm and a singlet corresponding to the $-OCH_3$ protons was also found at δ 3.76–3.81 ppm.[50]

For complexes **1** and **4**, a singlet observed at δ 8.26 and δ 7.95 ppm was attributed to the presence of the azomethine proton. However, for complexes **2** and **3**, a doublet appeared at δ 7.44 and δ 7.71 ppm, which may be due to the nuclear quadrupolar effect of the nitrogen atom.[51] In the spectra of complexes **2–4**, a singlet was observed at δ 9.69–11.12 ppm corresponding to the presence of the terminal –NH group of the coordinated ligand and in the spectrum of complex **1**, a triplet observed at δ 6.80 ppm was attributed to the presence of the terminal NH_2 protons.[52] For complexes **1** and **4**, a doublet appearing at δ 6.55 ppm and δ 6.18 ppm has been attributed to the presence of the NH proton of the triazole moiety. However, in the spectra of complexes **2** and **3**, a singlet was observed for the triazole –NH proton at δ 6.35 ppm and δ 6.38 ppm, which confirmed the participation of substituted triazole in coordination with the palladium ion.[53] The signal for the methyl proton was observed at δ 2.91 ppm as a singlet and at δ 1.26 ppm as a triplet for complexes **2** and **3**, respectively. In addition, the spectrum of **3** showed a multiplet at δ 2.88 ppm corresponding to the methylene protons.[24]

X-ray crystallography

The spectroscopy characterisation of complexes **2** and **4** gave some idea about the composition of the complexes, but they failed to indicate the definite binding mode of the thiosemicarbazone and the structures of the complexes. In order to confirm the exact structures, X-ray crystallographic studies were done for the new complexes (**2** and **4**). The ORTEP diagrams of the complexes are given in Fig. 1 and 2. The crystallographic data, selected bond distances and bond angles are listed in Tables 1 and 2. From the unit cell dimensions, it is clear that complex **2** crystallised in the monoclinic system with the space group P_12_1/C_1 (Fig. 1). In complex **2**, the palladium atom is coordinated through the phenolic oxygen, N1 hydrazinic nitrogen and thione sulphur atom by forming six member and five member rings and the fourth coordinate site is occupied by the sulphur atom of 5-(2-hydroxy-3-methoxy-phenyl)-4-methyl-2,4-dihydro[1,2,4]triazole-3-thione, which is formed by the cyclisation of $\mathbf{H_2L^2}$. The [Pd1–O2] bond distance (2.0175(19) Å),

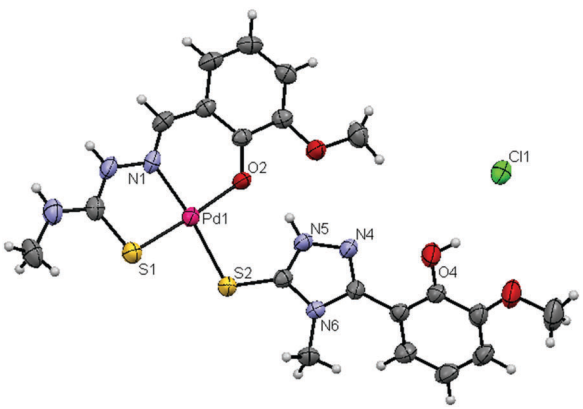

Fig. 1 ORTEP diagram of [Pd(H-Msal-mtsc)(Msal-mtaz)]·Cl (**2**) showing thermal ellipsoids at 50% probability level.

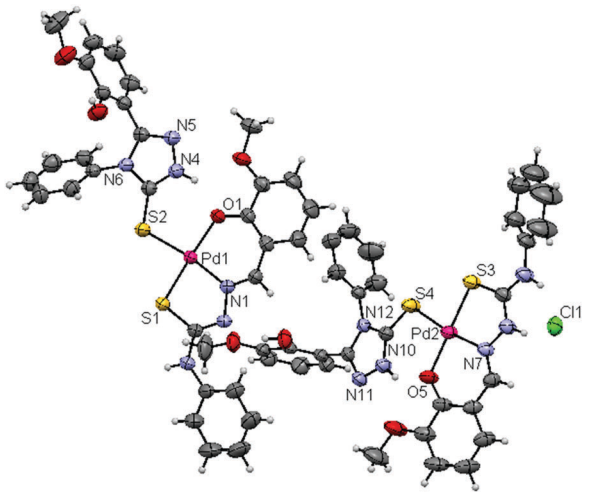

Fig. 2 ORTEP diagram of [Pd_2(Msal-ptsc)(Msal-ptaz)(H-Msal-ptsc)(Msal-ptaz)]·Cl (**4**) showing thermal ellipsoids at 50% probability level.

[Pd1–N1] bond distance (1.996(2) Å), [Pd1–S1] bond distance (2.2575(8) Å) and [Pd1–S2] bond distance (2.3322(8) Å) were found to be similar to the reported values.[24,48] The *trans* angles [N1–Pd1–S2] and [O2–Pd1–S1] were found to be 172.49(8) and 176.23(6), indicating the significant distortion of the square planar geometry around the palladium ion (Table 2).[48,54] The presence of a chloride ion outside the coordination sphere compensated the charge of palladium as Pd(II), resulting in the formation of an ionic complex. Complex **2** undergoes three intramolecular hydrogen bonding interactions through the hydrogen atom of the imine nitrogen of the triazole moiety (N5) with the phenolic oxygen atom (O2) having an N(5)–H(5)···O(2) distance of 2.580 Å and a hydrogen atom of the imine nitrogen N(5) of the triazole moiety with the methoxy oxygen atom (O1) having an N(5)–H(5)···O(1) distance of 2.883 Å and a hydrogen atom of the phenolic oxygen (O4) with the azomethine nitrogen (N4) atom having an O(4)–H(4)···N(4) distance of 2.966 Å (Table S1, ESI†). In addition, complex **2** undergoes two intermolecular hydrogen bonding interactions through the hydrogen atom of the phenolic oxygen atom (O4) with the chloride atom (Cl1) having an O(4)–H(4)···Cl(1) distance of 3.218 Å and the hydrogen atom of imine nitrogen (N2) with the chloride atom (Cl1) of the second molecule having an N(2)–H(2)···Cl(1) distance of 3.043 Å. The chloride atom bridged the two molecules through hydrogen bonding (Fig. S12, ESI†).

Complex **4** crystallised in the triclinic crystal system with the space group $P\bar{1}$. The crystal structure of **4** revealed that there are two independent mononuclear complexes in the single crystallographic unit. The crystal consists of one thiolate sulphur ONS complex and another thione sulphur ONS complex (Fig. 2). In complex **4**, the neutral Pd(II) complex unit, the palladium atom is coordinated through phenolic oxygen (O1), azomethine nitrogen (N1) and thiolate sulphur (S1) by forming six member and five member rings and the fourth coordinate site is occupied by the thione sulphur (S2) atom of 5-(2-hydroxy-3-methoxy-phenyl)-4-phenyl-2,4-dihydro[1,2,4]triazole-3-thione, which is formed by the cyclisation of $\mathbf{H_2L^4}$. The [Pd1–O2] bond distance

Table 1 Crystallographic data of complexes [Pd(H-Msal-mtsc)(Msal-mtaz)]·Cl (**2**) and [Pd_2(Msal-ptsc)(Msal-ptaz)(H-Msal-ptsc)(Msal-ptaz)]·Cl (**4**)

	[Pd(H-Msal-mtsc)(Msal-mtaz)]·Cl (2)	[Pd_2(Msal-ptsc)(Msal-ptaz)(H-Msal-ptsc)(Msal-ptaz)]·Cl (4)
Empirical formula	$C_{20}H_{23}N_6O_4PdS_2Cl$	$C_{60}H_{52}N_{12}O_8Pd_2S_4Cl$
Formula weight	614.41	1445.62
Temperature	293 K	293 K
Wavelength	0.71073 Å	0.71073 Å
Crystal system	Monoclinic	Triclinic
Space group	P_12_1/C_1	$P\bar{1}$
Unit cell dimension		
A	9.0019(3) Å	12.88650(10) Å
B	10.3208(3) Å	13.4398(2) Å
C	25.8409(9) Å	19.0250(3) Å
α	90°	74.7310°
B	94.137°	87.4550°
Γ	90°	84.5360°
Volume	2394.52(14) $Å^3$	3163.58(7) $Å^3$
Z	4	2
Density	1.713 Mg m^{-3}	1.518 Mg m^{-3}
Absorption coefficient	1.102 mm^{-1}	0.806 mm^{-1}
F(000)	1248	1466
Crystal size	0.12 × 0.07 × 0.02 mm	0.38 × 0.28 × 0.24 mm
Theta range for data collection	3.47 to 28.39°	3.17 to 24.71°
Index range	$11 \leq h \leq -11$, $13 \leq k \leq -13$, $31 \leq l \leq -33$	$15 \leq h \leq -15$, $15 \leq k \leq -15$, $22 \leq l \leq -22$
Reflection collected	10 154	70 651
Completeness to theta	24.66°	24.66°
Refinement method	Full-matrix least-squares on F^2	Full-matrix least-squares on F^2
Data/restraints/parameters	5543/0/312	10 769/36/778
Goodness of fit on F^2	1.035	1.064
Final *R* indices [$I > 2\ \sigma(I)$]	R_1 = 0.0720, wR_2 = 0.0647	R_1 = 0.0382, wR_2 = 0.0827
R indices (all data)	R_1 = 0.0403, wR_2 = 0.0729	R_1 = 0.0331, wR_2 = 0.0871

Table 2 Selected bond lengths (Å) and angels (°) for complexes **2** and **4**

	(2)	(4)
Bond lengths		
Pd1–S1	2.2575(8)	2.2386(7)
Pd1–S2	2.3322(8)	2.3238(8)
Pd1–O2	2.0175(19)	2.0288(18)
Pd1–N1	1.996(2)	1.992(2)
Pd2–S3	—	2.2537(8)
Pd2–S4	—	2.3135(8)
Pd2–O5	—	2.015(2)
Pd2–N7	—	1.984(2)
Bond angles		
S1–Pd1–S2	86.87(3)	86.95(3)
O2–Pd1–S2	96.58(6)	95.99(6)
N1–Pd1–S1	85.81(8)	84.56(7)
N1–Pd1–O2	90.78(9)	92.51(8)
O2–Pd1–S1	176.23(6)	177.04(6)
N1–Pd1–S2	172.49(8)	171.47(7)
S3–Pd2–S4	—	86.85(3)
O5–Pd2–S4	—	95.88(6)
N7–Pd2–S3	—	85.84(7)
N7–Pd2–O5	—	91.52(9)
O5–Pd2–S3	—	176.22(7)
N7–Pd2–S4	—	172.33(7)

(2.0288(18) Å), [Pd1–N1] bond distance (1.992(2) Å), [Pd1–S1] bond distance (2.2386(7) Å) and [Pd1–S2] bond distance (2.3238(8) Å) were found to be similar to the literature values.[24,48] However, in the ionic Pd(II) unit, the palladium atom is coordinated through phenolic oxygen (O5), azomethine nitrogen (N7) and thione sulphur (S3) by forming six member and five member rings. The remaining coordinate site is occupied by the thione sulphur (S4) atom of 5-(2-hydroxy-3-methoxy-phenyl)-4-phenyl-2,4-dihydro[1,2,4]triazole-3-thione, which is formed by the cyclisation of $\mathbf{H_2L^4}$. The [Pd2–O5] bond distance (2.015(2) Å), [Pd2–N7] bond distance (1.984(2) Å), [Pd1–S3] bond distance (2.2537(8) Å) and [Pd2–S4] bond distance (2.3135(8) Å) were found to be similar to the reported values.[24,54] The presence of a chloride ion outside the coordination sphere compensated the charge of palladium as Pd(II), resulting in the formation of an ionic complex unit. The elongation of the Pd(1)–S(2) and Pd(2)–S(4) bonds may be due to the strong *trans* influence of N(1) and N(7) nitrogen on thione sulphur–palladium. This is further evident from the shorter bond distance of the (1.701(3) Å) C16–S2 and (1.707(3) Å) C45–S4 bonds of the coordinated ligand.[55] The *trans* angles [N1–Pd1–S2] and [O1–Pd1–S1] were found to be 171.47(7)° and 177.04(6)° for the neutral complex unit and [N7–Pd2–S4] and [O5Pd2–S3] were found to be 172.33(7)° and 176.22(7)° for the ionic complex unit, respectively, which indicates the significant distortion around the square planar palladium ion (Table 2).[54]

The imine nitrogen of the triazole moiety in the neutral and ionic units in **4** is involved in two intramolecular hydrogen bonding with the phenolic oxygen atoms O(1) and O(5) of the salicylaldehyde thiosemicarbazone moiety, with N(4)–H(4)···O(1) and N(10)–H(10)···O(5) distances of 2.588 Å and 2.632 Å and another with the methoxy oxygen atoms O(2) and O(6) of the salicylaldehyde thiosemicarbazone moiety, with N(4)–H(4)···O(2) and N(10)–H(10)···O(6) distances of 2.908 Å and 2.919 Å. In the neutral unit, there is one intermolecular hydrogen bonding interaction between the phenolic oxygen O(3) atom and the chloride atom Cl(1) of the second molecule having an O(3)–H(3)···Cl(1) distance of 3.204 Å. In the ionic unit, there are two intermolecular hydrogen bonding interactions between the hydrogen atom of imine nitrogen N(8) and the chloride

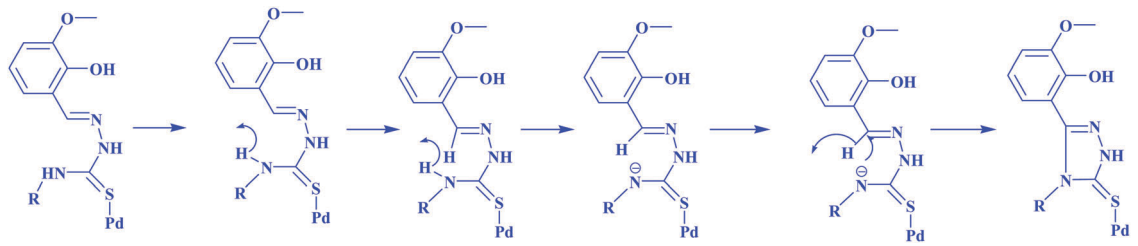

Scheme 2 The plausible mechanism of the formation of 5-(2-hydroxy-3-methoxy-phenyl)-2,4-dihydro-[1,2,4]triazole-3-thione derivatives.

atom Cl(1) having an N(8)–H(8)···Cl(1) distance of 3.055 Å and another hydrogen bonding interaction between the terminal nitrogen N(9) and the chlorine atom Cl(1) having an N(9)–H(9)···Cl(1) distance of 3.144 Å (Table S1, ESI†). In addition to these, an intramolecular hydrogen bonding interaction is observed between the hydrogen atom of the phenolic oxygen of the ionic unit and the imine nitrogen of the neutral unit with an O(7)–H(7)···N(2) distance of 2.909 Å (Fig. S13, ESI†).

Repeated attempts to get good quality crystals of complexes **1** and **3** suitable for the X-ray single crystallographic studies were unsuccessful. Hence, the stoichiometry of the complexes **1** and **3** were further confirmed by Electrospray Ionization Mass Spectroscopy (ESI-MS), the *m*/*z* value is 589.1237 and 645.2493 respectively (Fig. S14 and S15, ESI†).

A plausible mechanism for the formation of the 5-(2-hydroxy-3-methoxy-phenyl)-2,4-dihydro-[1,2,4]triazole-3-thione derivatives from the 3-methoxysalicylaldehyde thiosemicarbazones is given in Scheme 2.

DNA binding studies

Electronic absorption titration. The electronic absorption spectra of complexes **1–4** showed two to three absorption bands at 252–256 nm and 306–400 nm, which were assigned to the intra ligand transition (IL) and the ligand to metal charge transition (LMCT). The absorption spectra of complexes **1–4** at a constant concentration (10 μM) in the absence and presence of different concentrations of nucleotide CT-DNA (5–50 μM) are shown in Fig. 3. As the DNA concentration is increased, hyperchromism with small blue shifts of 2 nm and 1 nm (for **1**, **2** and **3**) and 4 nm (for **4**) was observed in the intra ligand band. The LMCT bands exhibited small hyperchromism without any shift for complexes **1**, **2** and **4** and a blue shift of 2 nm for complex **3**

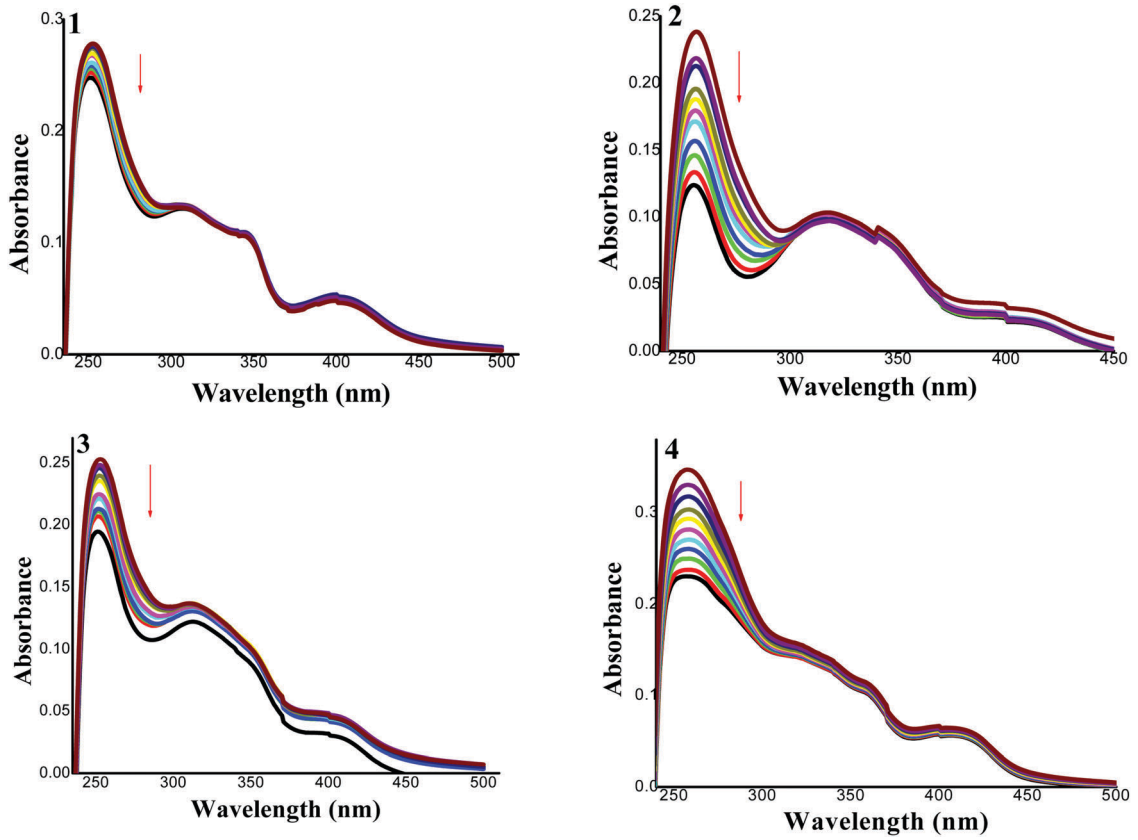

Fig. 3 Absorption titration of complexes **1–4** at a fixed concentration (10 μM) with increasing concentrations (5–50 μM) of CT-DNA (Tris–HCl, pH 7.2).

Table 3 The K_b (binding constant), K_{sv} (quenching constant) and K_{app} (apparent with EB) values for the interaction of complexes **1–4** with CT-DNA

Complex	K_b ($\times 10^5$ M^{-1})	K_{sv} ($\times 10^3$ M^{-1})	K_{app} ($\times 10^6$ M^{-1})
1	1.010 ± 0.10	1.86 ± 0.09	7.49
2	2.176 ± 0.12	2.61 ± 0.11	7.04
3	2.743 ± 0.15	4.14 ± 0.13	6.53
4	0.849 ± 0.09	1.53 ± 0.08	6.80

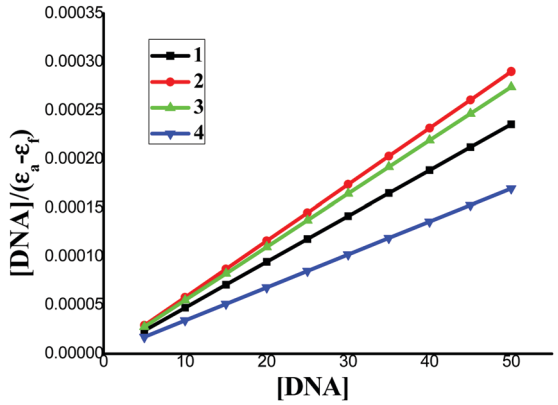

Fig. 4 Plot of [DNA] *versus* [DNA]/($\varepsilon_a - \varepsilon_f$).

was observed. The observed hyperchromism with a small blue shift implied that the complexes bind to DNA through the electrostatic binding mode.[56]

From the binding constant (K_b) values (Table 3 and Fig. 4), it is inferred that all the complexes bind with CT-DNA efficiently. Among the four complexes, complex **3** binds more strongly with CT-DNA compared to the remaining complexes. Based on the K_b value, we can arrange the complexes in the following order with respect to the electron donating ability of the ligand *i.e.* the substitution on the N-terminal nitrogen atom, **3** (ethyl) > **2** (methyl) > **1** (hydrogen) > **4** (phenyl).

Competitive studies with ethidium bromide. Ethidium bromide (EB) is a common fluorescent probe for DNA structure determination and has been employed in the examinations of the mode and process of binding of the metal complexes (**1–4**) to DNA. The fluorescent emission of EB bound to DNA in the absence and presence of Pd(II) complexes (**1–4**) is shown in Fig. 5. The emission intensity of EB–DNA decreased apparently as the concentration of the complexes (**1–4**) increased, which indicates that all the four complexes replaced EB from the EB–DNA system. Further, the apparent DNA binding constant (K_{app}) was calculated by using the following equation,

$$K_{EB}[EB] = K_{app}[complex]$$

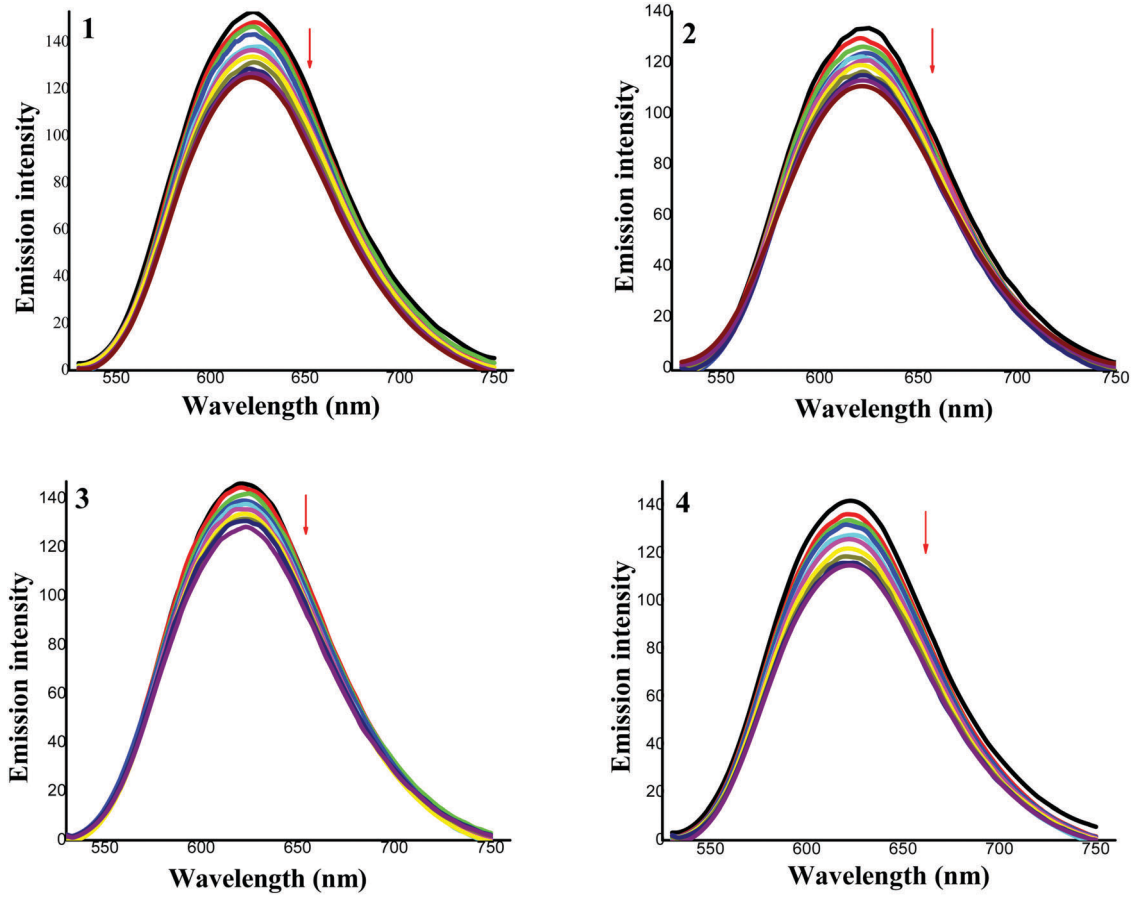

Fig. 5 Fluorescence quenching curves of ethidium bromide bound to DNA by complexes **1–4**. [DNA] = 10 μM, [EB] = 10 μM and [complex] = 0–100 μM.

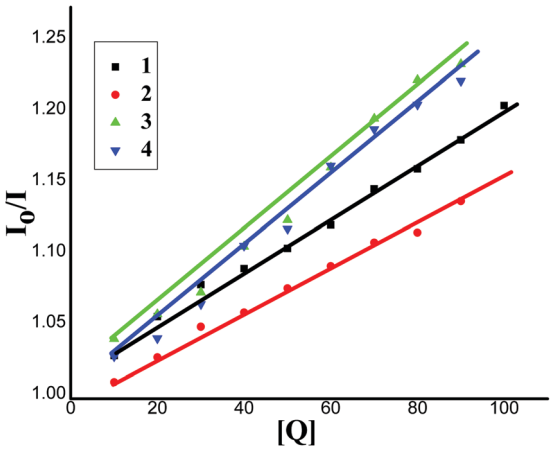

Fig. 6 Plot of [Q] *versus* I_0/I.

where the compound concentration is the value at 50% reduction in the fluorescence intensity of EB, K_{EB} (1.0×10^7 M^{-1}) is the DNA binding constant of EB, [EB] is the concentration of EB =10 μM. The calculated values of the quenching constant (K_{sv}) and apparent binding constant (K_{app}) are listed in Table 3. The determined quenching constants and binding constants of the complexes suggested an intercalative binding mode of the complexes to CT-DNA[57] (Table 3 and Fig. 6).

DNA cleavage. To assess the DNA cleavage ability of complexes **1–4**, supercoiled (SC) pBR322 DNA was incubated with 50 μM concentration of the complexes in 5 mM Tris–HCl/50 mM NaCl buffer at pH 7.2 for 2 h without the addition of a reductant (Fig. 7). Upon gel electrophoresis of the reaction mixture, DNA cleavage was observed, during which the SC DNA was converted into nicked circular (NC) DNA and linear DNA. The complexes did not require addition of any external agents to cleave the DNA. However, the metal precursors $K_2[PdCl_4]$, free ligands [H_2L^{1-4}] and 1,3-bis(diphenylphosphino)propane (dppp) did not show any appreciable cleavage activity. From this result, it is clear that the palladium(II) complexes (**1–4**) have the potential to cleave the supercoiled DNA and the new complexes (**1–4**) alone are responsible for the cleavage of the DNA.[58] Among the four complexes, complex **1** exhibited better DNA cleavage as compared to the other complexes. Moreover, in our complexes the possible cleavage mechanism was a hydrolytic cleavage mechanism.[59] While comparing the DNA binding profile of the complexes with the cleavage ability of them, it is concluded that the binding affinity and cleavage ability are not proportionate with each other.

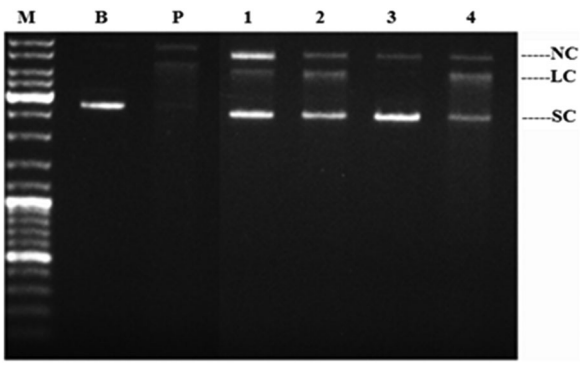

Fig. 7 Gel electrophoresis diagram showing the cleavage of the supercoiled pBR322 DNA by complexes **1–4** in 5% DMSO and 95% 5 mM Tris–HCl/50 mM NaCl buffer at pH 7.2 and at 37 °C with an incubation time of 2 h. Lane B: buffer + plasmid; Lane P: plasmid alone; Lane M: DNA ladder; Lane 1–4: complexes **1–4** (50 μM). Forms SC, NC, and LC are supercoiled, nicked, circular and linear circular DNA, respectively.

Protein binding studies

The interactions of drugs with plasma proteins particularly with serum albumin are very important to study, because binding to these proteins may lead to a loss or an improvement of the biological properties of the drugs or provide paths for drug transportation.[60]

UV absorption spectra of BSA. UV absorption spectroscopy is useful to distinguish between static and dynamic quenching, which is done by careful examination of the absorption spectra of BSA in the presence of complexes. The UV absorption spectra of BSA in the absence and presence of four complexes **1–4** showed that the absorption intensity of BSA enhanced when the compounds were added, and there was a blue shift in the wavelength for all the complexes (Fig. 8). The changes in the absorption spectra for the BSA + complexes indicated that the palladium(II) complexes interact with the BSA and we propose that the possible quenching mechanism of BSA by complexes followed static quenching.[61]

Fluorescence quenching studies of BSA. The interaction of BSA with the complexes (**1–4**) was studied by fluorescence measurements at room temperature. A solution of BSA (10 μM) was titrated with various concentrations of the complexes (0–70 μM). The effects of the complexes on the fluorescence emission spectra of BSA are shown in Fig. 9. The addition of the complexes (**1–4**) to a solution of BSA resulted in a significant decrease in the fluorescence intensity of BSA with a blue shift (Fig. 9). It is mainly because the active site in the protein is buried in a hydrophobic environment.[62] These results suggested a definite interaction of the complexes with the BSA protein.

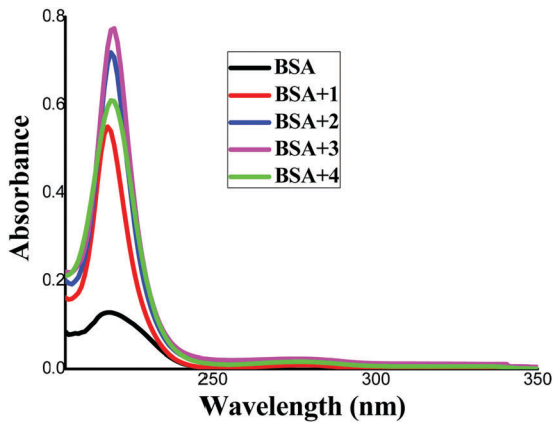

Fig. 8 UV absorption spectra of BSA (10 μM) in the absence and presence of the complexes.

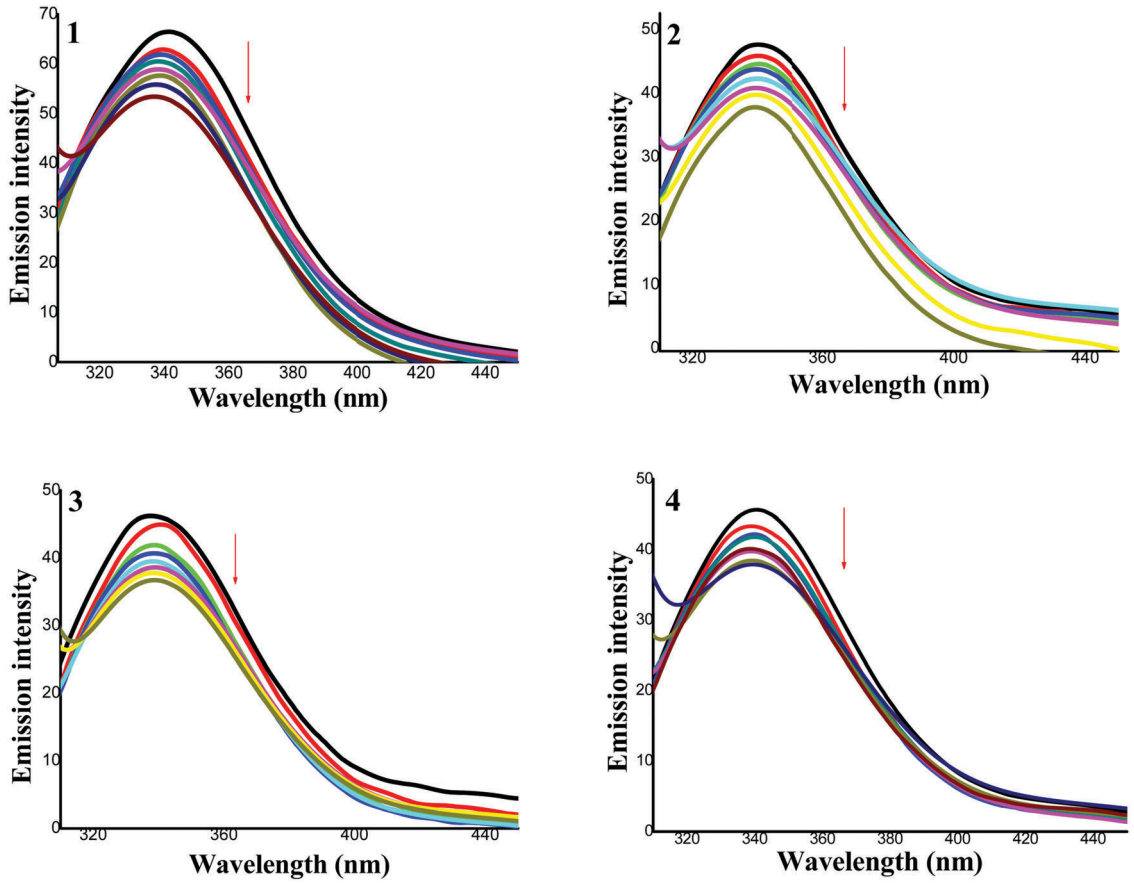

Fig. 9 Fluorescence quenching of BSA (1×10^{-6} M; λ_{exi} = 280; λ_{emi} = 346 nm) in the absence and presence of various concentrations of the complexes (0–70 μM).

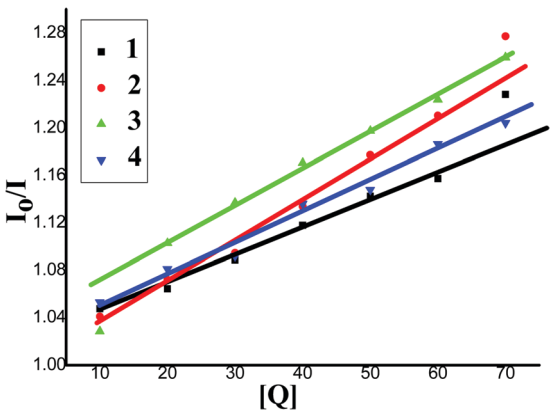

Fig. 10 Stern–Volmer plot of BSA.

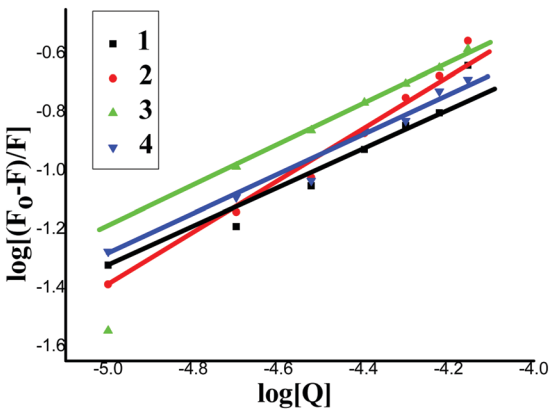

Fig. 11 Plot of log[Q] *vs.* log[($F_0 - F$)/F].

Fluorescence quenching data were further analysed with the Stern–Volmer equation and the Scatchard equation. The quenching constants (K_{sv}) were calculated from slope of the plot I_0/I *versus* [Q] the concentration of complexes (**1–4**), which resulted in a linear plot (Fig. 10). The observed linearity in the plots indicated the ability of the complexes to quench the emission intensity of BSA. The value of the binding constant (K_b) can be determined from the slope of the plot log[($F_0 - F$)/F] *versus* log[Q] (Fig. 11). The calculated values of the quenching constant (K_{sv}), binding constant (K_b) and the number of binding sites (n) are listed in Table 4. Complex **3** has a higher magnitude of binding than other complexes.

Synchronous fluorescence spectroscopic studies of BSA. A synchronous fluorescence spectroscopic study was used to obtain information about the molecular environment in the vicinity of the fluorophore moieties of BSA.[63] Synchronous

Table 4 Binding constant (K_b), quenching constant (K_{sv}) and number of binding sites (n) for the interaction of complexes (**1–4**) with BSA

Complex	K_b ($\times M^{-1}$)	K_{sv} ($\times 10^3$ M^{-1})	n
BSA + **1**	$3.10 \times 10^2 \pm 0.11$	2.74 ± 0.07	0.77 ± 0.05
BSA + **2**	$2.45 \times 10^3 \pm 0.15$	3.82 ± 0.11	0.96 ± 0.08
BSA + **3**	$7.72 \times 10^3 \pm 0.21$	3.56 ± 0.14	1.06 ± 0.09
BSA + **4**	$1.62 \times 10^2 \pm 0.13$	2.57 ± 0.10	0.71 ± 0.06

fluorescence spectra show the tyrosine residue of BSA only at a wavelength interval $\Delta\lambda$ of 15 nm, whereas the tryptophan residues of BSA at a $\Delta\lambda$ of 60 nm. When the concentration of the complexes (0–70 μM) added to BSA (10 μM) was increased, a decrease in the fluorescence intensity was observed for all the complexes in both tryptophan and tyrosine. However, the tryptophan spectra were accompanied by a blue shift (Fig. S16, ESI†) and revealed that the binding around the tryptophan residues was strengthened. These experimental results indicated that the metal complexes bind to the active site of the protein and brought a conformational change in the secondary structure of the protein.

Three dimensional fluorescence spectroscopy. Three-dimensional fluorescence spectroscopy has become a popular fluorescence analysis technique and it can provide more detailed information about the conformational changes of proteins. The conformational and micro environmental changes of BSA were investigated by comparing their spectral characteristics in the absence and presence of the complexes. The three-dimensional fluorescence spectra and the contour one are shown in Fig. 12. The normal fluorescence peaks are located in the lower right of the Rayleigh scattering regions.[64,65] Two typical fluorescence peaks could be found in the fluorescence spectra, which are marked as peaks 1 and 2. Peak 1 (λ_{exc} = 280.0 nm and λ_{emi} = 325.0 nm) mainly revealed the spectral behavior of the tryptophan and tyrosine residues, while peak 2 (λ_{exc} = 230.0 nm and λ_{emi} = 325.0 nm) may mainly exhibit the fluorescence emission characteristic of the polypeptide backbone structures (Table 5). As shown in Fig. 12, both of the fluorescence emission peaks in the three dimensional fluorescence spectra of BSA were quenched after the addition of the complexes, indicating that there were interactions between BSA and the complexes. The intensity changes of peaks 1 and 2 revealed that the binding of the complexes to BSA induced some conformational and micro-environment changes in BSA.[66]

Cytotoxicity studies

Cytotoxic activity against human tumour cell lines. The positive results obtained in the DNA binding, DNA cleavage and protein binding studies motivated us to evaluate the cytotoxicity of the complexes against MCF-7 human breast cancer cells using the colorimetric MTT assay (3-(4,5-dimethylthiazol-2-yl)-2,5-diphenyltetrazolium bromide). The cells were incubated

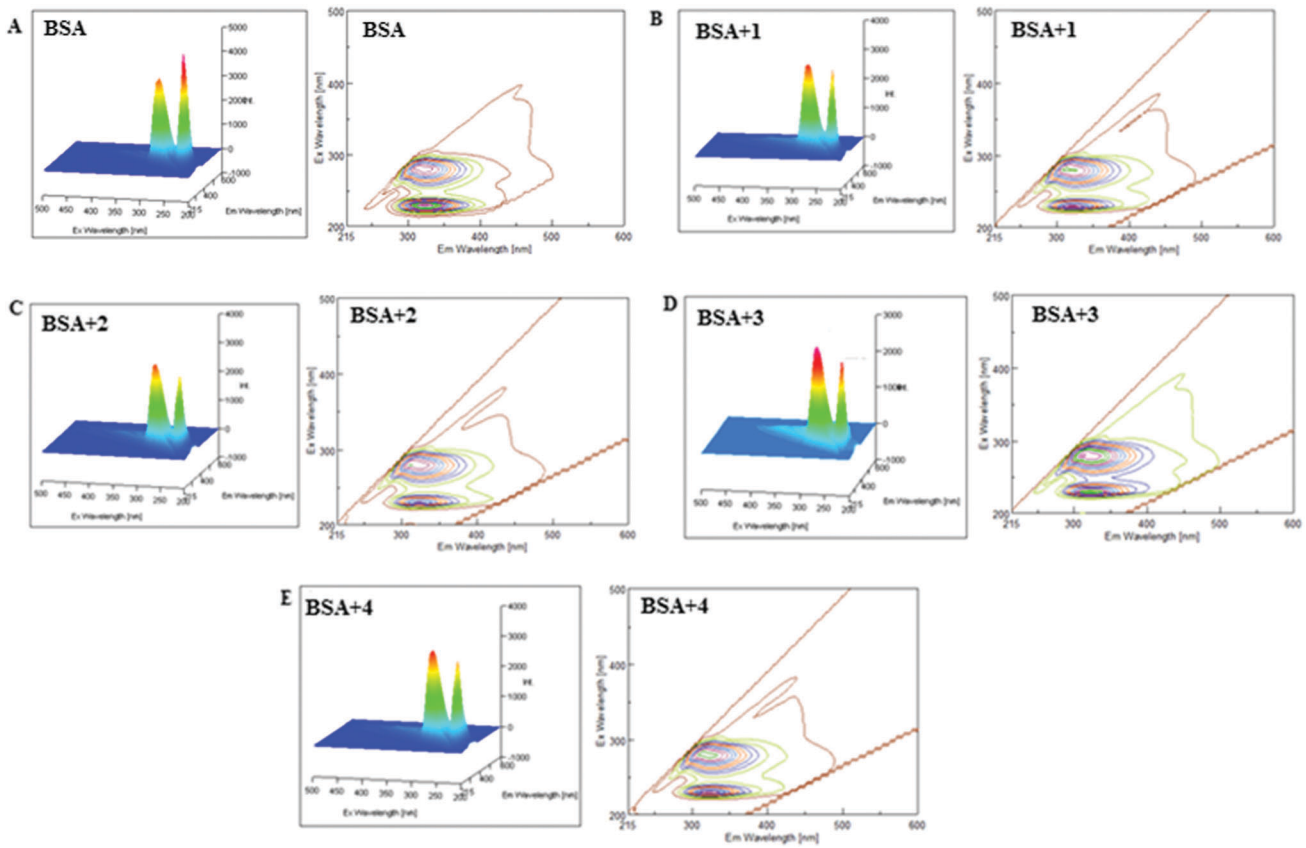

Fig. 12 The 3D fluorescence spectra of BSA (A) and BSA + **1** (B), BSA + **2** (C), BSA + **3** (D), and BSA + **4** (E).

Table 5 Three dimensional fluorescence spectral parameters for BSA in the absence and presence of palladium(II) complexes **1–4**

	Peak 1 (nm)			Peak 2 (nm)		
System	λ_{ex}	λ_{em}	$\Delta\lambda$	λ_{ex}	λ_{em}	$\Delta\lambda$
BSA	280	325	45	230	325	95
BSA + **1**	280	325	45	230	324	94
BSA + **2**	280	326	46	230	324	94
BSA + **3**	280	325	45	230	325	95
BSA + **4**	280	326	46	230	323	93

Table 6 *In vitro* cytotoxic activity of the compounds against the MCF-7 cell line expressed as IC_{50} values (μM). The results are expressed as the mean ± SD (n = 3)

	IC_{50} values (μM)
Compounds	MCF-7
Cisplatin	23.7 ± 0.07
$\mathbf{H_2L^1}$	>100
$\mathbf{H_2L^2}$	>100
$\mathbf{H_2L^3}$	>100
$\mathbf{H_2L^4}$	>100
$K_2[PdCl_4]$	>100
dppp	>100
1	9.50 ± 0.10
2	8.98 ± 0.07
3	5.60 ± 0.04
4	11.4 ± 0.11

with each compound for a period of 24 h and cisplatin was widely used as a standard. For an incubation period of 24 h, the new palladium(II) complexes exhibited a decrease in the cell viability and no substantial effect was observed in cell proliferation by the $K_2[PdCl_4]$, ligands, dppp, when compared with the control cells (Table 6). The inducing ability of the compounds was investigated by using the percentage of cell viability *versus* the concentration of compounds (Fig. S17, ESI†). It is important to mention that all the complexes (**1–4**) showed a better growth inhibitory effect than the well-known standard anticancer drug cisplatin with a IC_{50} value of 23.7 μM against the MCF-7 cell line.[21–23] Among the four complexes, complex **3** was the most effective with an IC_{50} value of 5.60 μM against MCF-7 as compared to the other complexes **1** (9.74 μM), **2** (8.98 μM) and **4** (11.48 μM). The observed cytotoxic effects of the new palladium(II) complexes towards the MCF-7 cell line were better than those of the previously reported palladium complexes.[24,25] The results observed for the cytotoxicity of the complexes are following a very similar trend, which was observed in the DNA/protein binding and antioxidant activity. In general, the Pd(II) complexes exhibited anticancer activity in the order of **3** > **2** > **1** > **4**.

Morphological analysis. The induction of apoptosis by chemotherapeutic agents has always been an ideal choice for the development of new anticancer therapeutics. Therefore, we examined the induction of apoptosis, for which MCF-7 cells were treated with different concentrations of palladium(II) complexes (**1–4**) and were observed under phase inverted microscopy. The untreated cells were normal in size and shape.

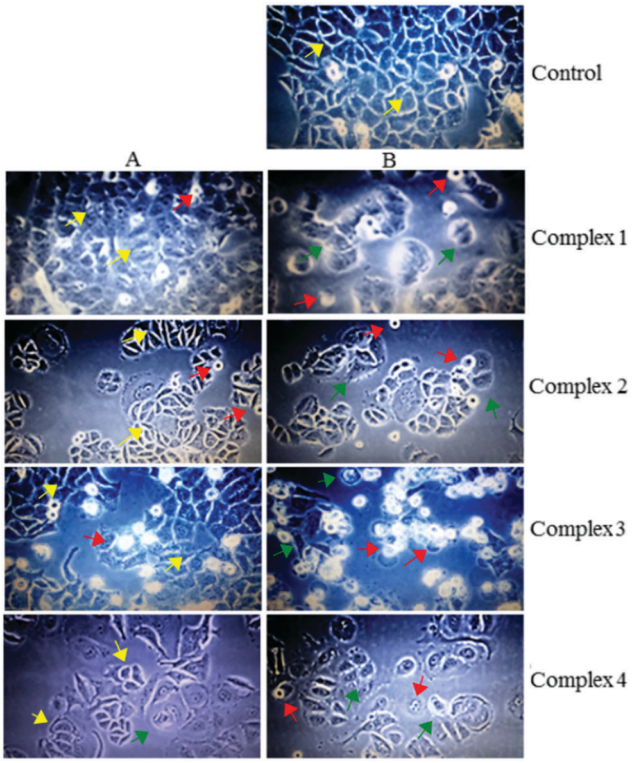

Fig. 13 Morphological changes induced by complexes **1–4** treated with breast cancer cells. The MCF-7 cells were treated with complexes **1–4** (6.25 μM and 12.5 μM) for 24 h and the cells were visualized under inverted microscopy (100×) to investigate the morphological alteration. Yellow arrows show the normal cells, red arrows indicate nuclear condensation and cell shrinkage and green arrows indicate membrane blebbing, cell deformation or abnormal cell shape. In this figure, (A and B) show the MCF-7 treated cells with 6.25 μM and 12.5 μM concentrations of the complexes.

In contrast, the complex treated cells exhibited morphological changes predominantly cell shrinkage, membrane blebbing and nuclear condensation, which are shown in Fig. 13. These changes correspond to the apparent characteristic of cell apoptosis[67] and implied that the growth inhibitory effect of the palladium(II) complexes might result from their apoptosis inducing activity.

Apoptosis study. Apoptosis studies were performed by a staining method using acridine orange (AO) and ethidium bromide (EB) to identify the difference in the membrane integrity between necrosis and apoptosis. AO can pass through the cell membrane of living and apoptotic cells, while staining by EB indicate the loss of membrane integrity. Under a fluorescence microscope, the living cells appear green, the necrotic cells appear red and the apoptosis cells appear greenish yellow or orange and morphological changes such as membrane blebbing, nuclear shrinkage will be observed. After 24 h treatment, complexes **2** and **3** showed membrane blebbing, cell shrinkage, condensed and fragmented nuclei in the MCF-7 cell lines, which are characteristic of early apoptosis (yellow fluorescence) and late apoptosis (orange red fluorescence)[68,69] (Fig. 14). In contrast, the control cells showed a green intact nuclear

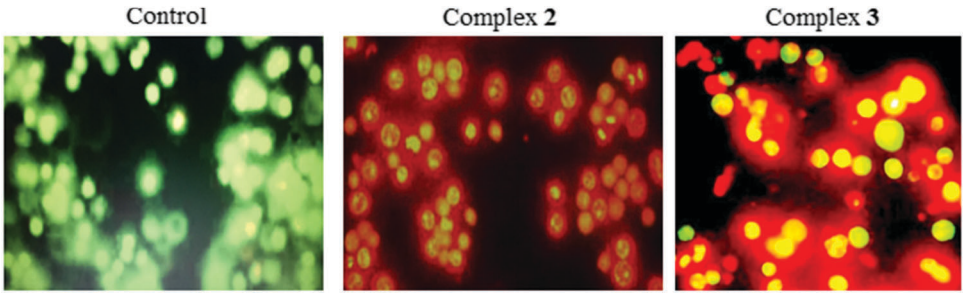

Fig. 14 Fluorescence images of the MCF-7 cells treated with an IC_{50} concentration of complexes **2** and **3** and the cells were stained with AO/EB for 24 h.

structure and a good cellular morphology. From these results, we concluded that complexes **2** and **3** induced the apoptosis in the MCF-7 cancer cells.

Conclusions

New palladium(II) complexes were synthesised and characterised by various spectral and analytical techniques. Further, the exact structures of complexes **2** and **4** were confirmed by X-ray crystallographic studies. Complex **2** is a mononuclear complex with ONS chelation of the ligand and the fourth site was occupied by the thione sulphur atom of 5-(2-hydroxy-3-methoxy-phenyl)-4-methyl-2,4-dihydro[1,2,4]triazole-3-thione, which is formed by the cyclization of $\mathbf{H_2L^2}$. The presence of a chloride ion outside the coordination sphere compensated the charge of palladium as Pd(II), resulting in the formation of an ionic complex. Whereas, complex **4** contains two independent units in the single crystallographic unit cell. The palladium atom with the neutral unit shows ONS chelation of the ligand and the fourth coordinate site was occupied by the thione sulphur atom of 5-(2-hydroxy-3-methoxy-phenyl)-4-phenyl-2,4-dihydro[1,2,4]-triazole-3-thione and in the second unit, the palladium ion coordinated with the ligand as a monobasic tridentate donor and thione sulphur bonded 5-(2-hydroxy-3-methoxy-phenyl)-4-phenyl-2,4-dihydro[1,2,4]triazole-3-thione, which is formed through the cyclization of $\mathbf{H_2L^4}$. The chloride ion is present outside the coordination sphere for the charge compensation of the palladium ion. From the result of the DNA binding studies, it is concluded that the complexes exhibited significant binding affinity and the interaction of the complexes with DNA is through electrostatic interaction. All the complexes cleaved supercoiled DNA without any external agents. The fluorescence quenching experiments with BSA confirmed the binding ability of the complexes and the static type of quenching. In addition, the synchronous and 3D fluorescence spectral investigations revealed that the complexes induced a small change in the secondary structure of the protein. The *in vitro* cytotoxicity of the compounds was evaluated against the MCF-7 (human breast cancer) cell line by comparing with cisplatin and complexes **2** and **3** exhibited significant cytotoxicity. Morphological analysis was performed using inverted phase contrast and fluorescence microscopes by AO/EB staining assay, which showed that complexes **2** and **3** were able to prompt the cell death of the human MCF-7 breast cancer cells through apoptosis. There is a correlation between the DNA binding and the cytotoxicity of the complexes, proving that complexes **2** and **3** can be better candidates for use as anticancer drugs.

Conflicts of interest

There are no conflicts to declare.

Acknowledgements

The author A. S. gratefully acknowledges the University Grants Commission (UGC), New Delhi for a UGC-BSR Fellowship, New Delhi, India [Grand No. G2/14308/17750/UGC BSR/Selection Comt./2014 dt.15.09.2014].

References

1 A. R. Kapdi and I. J. S. Fairlamb, *Chem. Soc. Rev.*, 2014, **43**, 4751–4777.
2 A. Garoufis, S. K. Hadjikakou and N. Hadjiliadis, *Coord. Chem. Rev.*, 2009, **253**, 1384–1397.
3 M. D. Coskun, F. Ari, A. Y. Oral, M. Sarimahmut, H. M. Kutlu, V. T. Yilmaz and E. Ulukaya, *Bioorg. Med. Chem.*, 2013, **21**, 4698–4705.
4 G. Gasser, I. Ott and N. M. Nolte, *J. Med. Chem.*, 2011, **54**, 3–25.
5 B. B. Zmejkovski, A. Savic, J. Poljarevic, N. Pantelic, N. A. Elovic, S. Radulovic, G. N. Kaluderovic and T. J. Sabo, *Polyhedron*, 2014, **80**, 106–111.
6 D. Aguila, E. Escribano, S. Speed, D. Talancon, L. Yerman and S. Alvarez, *Dalton Trans.*, 2009, 6610–6625.
7 A. L. Gavrilova and B. Bosnich, *Chem. Rev.*, 2004, **104**, 349–383.
8 (*a*) T. S. Lobana, R. Sharma, G. Bawa and S. Khanna, *Coord. Chem. Rev.*, 2009, **253**, 977–1055; (*b*) T. S. Lobana, G. Bawa, A. Castineiras, R. J. Butcher and M. Zeller, *Organometallics*, 2008, **27**, 175–180.
9 R. Archaryya, F. Basuli, S. M. Peng, G. H. Lee, L. R. Falvello and S. Bhattacharya, *Inorg. Chem.*, 2006, **45**, 1252–1259.
10 I. Pal, F. Basuli, T. C. W. Mak and S. Bhattacharya, *Angew. Chem., Int. Ed.*, 2001, **40**, 2923–2925.

11 V. Kaur, J. S. Aulakh and A. K. Malik, *Anal. Chim. Acta*, 2007, **603**, 44–50.
12 N. Cutillas, G. S. Yellol, C. De Haro, C. Vicente, V. Rodriguez and J. Ruiz, *Coord. Chem. Rev.*, 2013, **257**, 2784–2797.
13 S. Medici, M. Peana, V. M. Nurchi, J. I. Lachowicz, G. Crisponi and M. A. Zoroddu, *Coord. Chem. Rev.*, 2015, **284**, 329–350.
14 J. S. Casas, M. V. Castano, E. E. Castellano, J. Ellena, M. S. G. Tasende, A. A. Gato, A. Snchez, L. M. Sanjuan and J. Sordo, *Inorg. Chem.*, 2002, **41**, 1550–1557.
15 J. S. Casas, M. S. G. Tasende and J. Sordo, *Coord. Chem. Rev.*, 2000, **209**, 197–261.
16 T. S. Lobana, R. Sharma, G. Bawa and S. Khanna, *Coord. Chem. Rev.*, 2009, **253**, 997–1055.
17 A. G. Quiroga and C. N. Ranninger, *Coord. Chem. Rev.*, 2004, **248**, 119–133.
18 H. Beraldo and D. Gambino, *Mini-Rev. Med. Chem.*, 2004, **4**, 31–39.
19 S. Halder, S. M. Peng, G.-H. Lee, T. Chatterjee, A. Mukherjee, S. Dutta, U. Sanyal and S. Bhattacharya, *New J. Chem.*, 2008, **32**, 105–114.
20 D. K. Demertzi, M. A. Demertzis, J. R. Miller, C. Papadopoulou, C. Dodorou and G. Filousis, *J. Inorg. Biochem.*, 2001, **86**, 555–563.
21 W. Hernandez, A. J. Vaisberg, M. Tobar, M. Alvarez, J. Manzur, Y. Echevarria and E. Spodine, *New J. Chem.*, 2016, **40**, 1853–1860.
22 A. I. Matesanz, J. Perles and P. Souza, *Dalton Trans.*, 2012, **41**, 12538–12547.
23 A. A. Ibrahim, H. Khaledi, P. Hassandarvish, H. Mohd Alia and H. Karimian, *Dalton Trans.*, 2014, **43**, 3850–3960.
24 P. Kalaivani, R. Prabhakaran, E. Ramachandran, F. Dallemer, G. Paramaguru, R. Renganathan, P. Poornima, V. Vijaya Padma and K. Natarajan, *Dalton Trans.*, 2012, **41**, 2486–2499.
25 P. Kalaivani, R. Prabhakaran, F. Dallemer, P. Poornima, E. Vaishnavi, E. Ramachandran, V. Vijaya Padma, R. Renganathan and K. Natarajan, *Metallomics*, 2012, **4**, 101–113.
26 S. M. Hecht and W. O. Foye, *Cancer Chemother. Agents*, 1995, **34**, 369–388.
27 S. J. Franklin, *Curr. Opin. Chem. Biol.*, 2001, **5**, 201–208.
28 T. D. Maurer, B. J. Kraft, S. M. Lato, A. D. Ellington and J. M. Zaleski, *Chem. Commun.*, 2000, 69–70.
29 E. Meggers, *Chem. Commun.*, 2009, 1001–1010.
30 Q. Saquib, A. A. Al-Khedhairy, S. Al-Arifi, A. Dhawan and J. Musarrat, *Toxicol. In Vitro*, 2009, **23**, 848–854.
31 S. Purohit, A. P. Koley, L. S. Prsad, P. T. Manoharan and S. Ghosh, *Inorg. Chem.*, 1989, **28**, 3735–3742.
32 Y. Guo, K. Fhayli, S. Li, Y. Yang, A. Mashat and N. M. Khashab, *RSC Adv.*, 2013, **3**, 17693–17695.
33 A. L. Vogel, *Text Book of Practical Organic Chemistry*, Longman, London, 5th edn, 1989, p. 268.
34 R. H. Blessing, *Acta Crystallogr., Sect. A: Found. Crystallogr.*, 1995, **51**, 33–38.
35 G. M. Sheldrick, *SHELXTL Version 5.1 "An Integrated System for Solving, Refining and Displaying Crystal Structures from Diffraction Data"*, Siemens Analytical X-ray Instruments, Madison WI, 1990.
36 G. M. Sheldrich, *SHELXTYL-97, Program for Refinement of Crystal Structures*, University of Gottingen, Germany, 1997.
37 S. Sathiyaraj, K. Sampath, R. J. Butcher, R. Pallepogu and C. Jayabalakrishnan, *Eur. J. Med. Chem.*, 2013, **64**, 81–89.
38 T. Mossman, *J. Immunol. Methods*, 1983, **65**, 55–63.
39 H. J. Motulsky, *Prism 5 Statistics Guide*, GraphPad Software Inc., San Diego, CA, 2007, http://www.graphpad.com.
40 P. Moongkarndi, N. Kosem, S. Kaslungka, O. Luanratana, N. Pongpan and N. Neungton, *J. Ethnopharmacol.*, 2004, **90**, 161–166.
41 A. Gohel, M. B. McCarthy and G. Gronowicz, *Endocrinology*, 1999, **140**, 5339–5347.
42 T. B. Demirci, G. Congur, A. Erdem, S. E. Kuruca, N. Ozdemir, K. Akgun-Dar, B. Varol and B. Ulkuseven, *New J. Chem.*, 2015, **39**, 5643–5653.
43 R. Prabhakaran, P. Kalaivani, R. Huang, P. Pornima, V. Vijaya Padma and K. Natarajan, *J. Biol. Inorg. Chem.*, 2013, **18**, 233–247.
44 K. Alomar, M. A. Khan, M. Allain and G. Bouet, *Polyhedron*, 2009, **28**, 1273–1280.
45 P. Kalaivani, R. Prabhakaran, F. Dallemer and K. Natarajan, *RSC Adv.*, 2014, **4**, 51850–51864.
46 A. A. Ali, H. Nimir, C. Aktas, V. Huch, U. Rauch and K. H. Schafer, *Organometallics*, 2012, **31**, 2256–2262.
47 W. Su, Q. Qian, P. Li, X. Lei, Q. Xiao, S. Huang, C. Huang and J. Cui, *Inorg. Chem.*, 2013, **52**, 12440–12449.
48 P. Kalaivani, C. Umadevi, R. Prabhakaran, F. Dallemer and P. S. Mohan, *Inorg. Chim. Acta*, 2015, **438**, 264–276.
49 R. Prabhakaran, R. Sivasamy, J. Angayarkanni, R. Huang, P. Kalaivani, R. Karvembu, F. Dallemer and K. Natarajan, *Inorg. Chim. Acta*, 2011, **374**, 647–653.
50 R. Prabhakaran, P. Kalaivani, P. Poornima, F. Dallmer, G. Paramaguru, V. Vijay Padma, V. Renganathan and K. Natarajan, *Dalton Trans.*, 2012, **41**, 9323–9336.
51 D. Jayita, D. Sayanti, S. Dipravath Kumar and S. Bhattacharya, *RSC Adv.*, 2012, **2**, 11751–11763.
52 F. J. Bullock and D. Jardetsky, *J. Org. Chem.*, 1964, **29**, 1988–1990.
53 C. Rodrigues, A. A. Batista, R. Q. Aucelio, L. R. Teixeira, L. C. Visentin and H. Beraldo, *Polyhedron*, 2008, **27**, 3061–3066.
54 P. Chellan, K. M. Land, A. Shokar, A. Au, A. Hwan Au, C. M. Clavel, P. J. Dyson, C. D. Kock, P. J. Smith, K. Chibale and G. S. Smith, *Organometallics*, 2012, **31**, 5791–5799.
55 W. Hernandez, J. Paz, F. Carrasco, A. Vaisberg, E. Spodine, J. Manzur, L. Hennig, J. Sieler, S. Blaurock and L. Beyer, *Bioinorg. Chem. Appl.*, 2013, **2013**, 1–12.
56 E. C. Long and J. K. Barton, *Acc. Chem. Res.*, 1990, **23**, 271–273.
57 P. Kalaivani, R. Prabhakaran, M. V. Kaveri, R. Huang, R. J. Staples and K. Natarajan, *Inorg. Chim. Acta*, 2013, **405**, 415–426.
58 M. Muralisanker, N. S. P. Bhuvanesh and A. Sreekanth, *New J. Chem.*, 2016, **40**, 2661–2679.
59 K. R. SangeethaGowda, B. B. Mathew, C. N. Sudhamani and H. S. BhojyaNaik, *Biomed. Biotechnol.*, 2014, **2**, 1–9.

60 C. Tan, J. Liu, H. Li, W. Zheng, S. Shi, L. Chen and L. Ji, *J. Inorg. Biochem.*, 2008, **102**, 347–358.
61 Y. Z. Zhang, H. R. Li, J. Dai, W. J. Chen, J. Zhang and Y. Liu, *Biol. Trace Elem. Res.*, 2010, **135**, 136–152.
62 G. Prakash, R. Manikandan, P. Viswanathamurthi, K. Velmurugan and R. Nandhakumar, *J. Photochem. Photobiol., B*, 2014, **138**, 63–74.
63 N. Wang, L. Ye, B. Q. Zhao and J. X. Yu, *Braz. J. Med. Biol. Res.*, 2008, **41**, 589–595.
64 Y. Z. Zhang, B. Zhou, Y. X. Liu, C. X. Zhou, X. L. Ding and Y. Liu, *J. Fluoresc.*, 2008, **18**, 109–118.
65 X. L. Han, P. Mei, Y. Liu, Q. Xiao, F. L. Jiang and R. Li, *Spectrochim. Acta, Part A*, 2009, **74**, 781–787.
66 J. Juarez, S. G. Lopez, A. Cambon, P. Taboada and V. Mosquera, *J. Phys. Chem. B*, 2009, **113**, 10521–10529.
67 U. Lewandowska, K. Szewczyk, K. Owczarek, Z. Hrabec, A. Podsedek, M. Koziolkiewicz and E. Hrabec, *J. Agric. Food Chem.*, 2013, **61**, 2987–2998.
68 T. Suzuki, K. Fujikura, T. Higashiyama and K. Takata, *J. Histochem. Cytochem.*, 1997, **45**, 49–53.
69 G. Ciapetti, D. Granchi, L. Savarino, E. Cenni, E. Magrini, N. Baldini and A. Giunti, *Biomaterials*, 2002, **23**, 617–627.

